

Calculation of nuclear magnetic resonance shieldings using frozen-density embedding

Christoph R. Jacob and Lucas Visscher

Citation: *J. Chem. Phys.* **125**, 194104 (2006); doi: 10.1063/1.2370947

View online: <http://dx.doi.org/10.1063/1.2370947>

View Table of Contents: <http://jcp.aip.org/resource/1/JCPSA6/v125/i19>

Published by the [American Institute of Physics](http://www.aip.org).

Additional information on *J. Chem. Phys.*

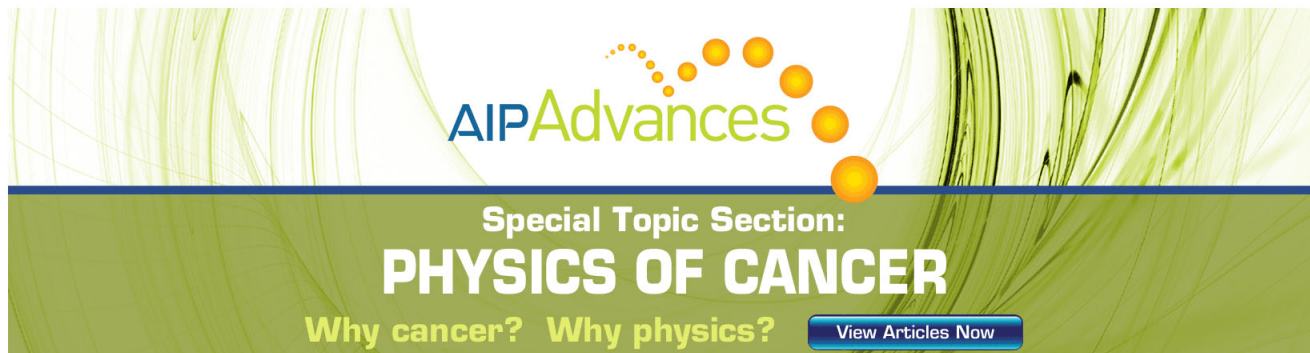
Journal Homepage: <http://jcp.aip.org/>

Journal Information: http://jcp.aip.org/about/about_the_journal

Top downloads: http://jcp.aip.org/features/most_downloaded

Information for Authors: <http://jcp.aip.org/authors>

ADVERTISEMENT



AIPAdvances

Special Topic Section:
PHYSICS OF CANCER

Why cancer? Why physics? [View Articles Now](#)

Calculation of nuclear magnetic resonance shieldings using frozen-density embedding

Christoph R. Jacob^{a)} and Lucas Visscher^{b)}

Faculty of Sciences, Department of Theoretical Chemistry, Vrije Universiteit Amsterdam, De Boelelaan 1083, 1081 HV Amsterdam, The Netherlands

(Received 8 September 2006; accepted 28 September 2006; published online 16 November 2006)

We have extended the frozen-density embedding (FDE) scheme within density-functional theory [T. A. Wesolowski and A. Warshel, *J. Phys. Chem.* **97**, 8050 (1993)] to include external magnetic fields and applied this extension to the nonrelativistic calculation of nuclear magnetic resonance (NMR) shieldings. This leads to a formulation in which the electron density and the induced current are calculated separately for the individual subsystems. If the current dependence of the exchange-correlation functional and of the nonadditive kinetic-energy functional are neglected, the induced currents in the subsystems are not coupled and each of them can be determined without knowledge of the induced current in the other subsystem. This allows the calculation of the NMR shielding as a sum of contributions of the individual subsystems. As a test application, we have calculated the solvent shifts of the nitrogen shielding of acetonitrile for different solvents using small geometry-optimized clusters consisting of acetonitrile and one solvent molecule. By comparing to the solvent shifts obtained from supermolecular calculations we assess the accuracy of the solvent shifts obtained from FDE calculations. We find a good agreement between supermolecular and FDE calculations for different solvents. In most cases it is possible to neglect the contribution of the induced current in the solvent subsystem to the NMR shielding, but it has to be considered for aromatic solvents. We demonstrate that FDE can describe the effect of induced currents in the environment accurately. © 2006 American Institute of Physics.
[DOI: [10.1063/1.2370947](https://doi.org/10.1063/1.2370947)]

I. INTRODUCTION

Nuclear magnetic resonance (NMR) spectroscopy is one of the most important and powerful tools in chemistry and biochemistry and quantum-chemical calculations of NMR parameters have developed into a routine task (for reviews, see Refs. 1 and 2). Often these calculations assist in the assignment of NMR spectra and their interpretation (see, e.g., Refs. 3–7). Due to its ease of application and computational efficiency, density-functional theory (DFT) is the standard method for the calculation of NMR parameters.

In the past years, there is an increasing interest in quantum-chemical calculations of NMR parameters for large systems (with a few hundred atoms), e.g., biological systems or molecules in solution or in other complex environments, and methods that show a linear scaling with the system size have been implemented for the Hartree-Fock and DFT calculations of NMR parameters.^{8,9} However, even with linear scaling of the computational effort these methods still have high computational requirements for many systems of interest, since they require a full quantum-mechanical treatment of the whole system.

The NMR shielding describes the induced current near the NMR active nucleus, with the nuclear magnetic moment acting as a probe. Because the operator corresponding to this nuclear magnetic moment is relatively short ranged, scaling

as r^{-2} with the distance r to the nucleus, the NMR shielding can be regarded as a rather “near-sighted” property. Therefore, it is often possible to focus on a subsystem that is close to the NMR active nucleus, avoiding the quantum-mechanical treatment of the full system. One possible way of exploiting this near sightedness of the NMR shielding are methods that treat only a small part of the system containing the NMR active nuclei explicitly quantum mechanically, while a more approximate method is chosen to represent the environment. The most prominent example of methods following this strategy are combined quantum mechanics / molecular mechanics (QM/MM) methods.^{10,11} However, the success of QM/MM methods relies on the careful parametrization of the force field used in the MM part.

For the special case that the environment is formed by a solvent, continuum solvation models, in which the solvent environment is described as a continuous medium characterized by its dielectric constant, can be employed for the calculation of NMR parameters.^{12–14} While it is clear that continuum models are able to correctly describe unspecific solvent effects, i.e., dielectric medium effects, problems may appear in the description of specific effects such as hydrogen bonding. Especially for the calculation of NMR shieldings it has been found that it is necessary to combine the continuum description with the explicit inclusion of a number of solvent molecules.^{15–17}

Frozen-density embedding (FDE), originally introduced by Wesolowski and Warshel,^{18,19} offers an appealing alterna-

^{a)}Electronic mail: jacob@few.vu.nl

^{b)}Electronic mail: visscher@chem.vu.nl

tive for the DFT calculation of NMR shieldings in large systems. The FDE scheme is based on a partitioning into separate subsystems, which are each calculated separately, with the effect of the other (frozen) subsystems represented by an effective embedding potential which only depends on their charge density. Even though the construction of this embedding potential requires the use of an approximate kinetic-energy functional, the FDE scheme itself is in principle exact. It thus allows it to exploit the near sightedness of the NMR shielding by focusing on the subsystem containing the NMR active nuclei while still keeping the quantum-mechanical treatment of the full system.

The FDE scheme has been successfully applied for the calculation of various molecular properties of systems in large environments.^{20,21} In particular, it has been applied to modeling solvation effects on electronic absorption spectra^{22,23} and on electron spin resonance (ESR) hyperfine coupling constants.²⁴ In these studies, the required charge density of the solvent was obtained using further approximations, such as using a sum of molecular fragments, which makes it possible to calculate the molecular properties for a large number of snapshots obtained from molecular dynamics simulations and to consider clusters consisting of a few hundred atoms in each snapshot. FDE has also been used to describe more complex environments, e.g., for studying induced circular dichroism in guest-host systems.²⁵

The FDE scheme has also been applied to free energy calculations in solution and biological environments.^{26,27} Furthermore, Iannuzzi *et al.* have made use of FDE for molecular dynamics simulations,²⁸ and the same embedding potential as in FDE was employed by Carter and co-workers,^{29–34} in an “*ab initio* in DFT” embedding approach combining a wave-function-based treatment of an atom or molecule absorbed on a surface with a periodic DFT description of the surface.

In this work, we will extend the FDE formalism to the calculation of NMR shieldings and test the method for the calculation of solvent shifts of NMR shieldings, using small solute-solvent clusters.

This work is organized as follows. First, we will present the theory of the calculation of NMR shieldings using frozen-density embedding in Sec. II. After a brief review of nonrelativistic current density-functional theory in Sec. II A and of the nonrelativistic DFT calculation of NMR shieldings in Sec. II B, we present the theory of frozen-density embedding for systems in magnetic fields in Sec. II C. This theory is then applied to the calculation of NMR shieldings using FDE in Sec. II D. In Sec. III computational details are given, and in Sec. IV, the FDE formalism is applied to the calculation of the solvent shift of the nitrogen NMR shielding in acetonitrile. Concluding remarks follow in Sec. V.

II. THEORY

A. Nonrelativistic current density-functional theory

The starting point for the nonrelativistic DFT calculation of NMR shieldings is the generalization of DFT to include magnetic fields, which is given by current density-functional theory (CDFT) as it was first formulated for closed-shell sys-

tems by Vignale and Rasolt.³⁵ This requires to consider not only the electron density $\rho(\mathbf{r})$ as the basic variable but also the current density $\mathbf{j}(\mathbf{r})$. They show that in order to prove an analog of the Hohenberg-Kohn theorem, it is necessary to use the electron density $\rho(\mathbf{r})$ and the paramagnetic current $\mathbf{j}_p(\mathbf{r}) = \mathbf{j}(\mathbf{r}) + \rho(\mathbf{r})\mathbf{A}(\mathbf{r})$ as basic variables, i.e., the (gauge-dependent) paramagnetic current \mathbf{j}_p has to be used instead of the (gauge-invariant) total current \mathbf{j} .^{35,36}

In the following, we will always consider a closed-shell system with N doubly occupied orbitals and with $2N$ electrons. For such a system in an external magnetic field the total energy functional is given by

$$E[\rho, \mathbf{j}_p] = T_s[\rho, \mathbf{j}_p] + \int v_{\text{nuc}}(\mathbf{r})\rho(\mathbf{r})d\mathbf{r} - \int \mathbf{j}_p(\mathbf{r})\mathbf{A}(\mathbf{r})d\mathbf{r} + \frac{1}{2} \int \rho(\mathbf{r})A^2(\mathbf{r})d\mathbf{r} + \int \frac{\rho(\mathbf{r})\rho(\mathbf{r}')}{|\mathbf{r} - \mathbf{r}'|}d\mathbf{r} + E_{\text{xc}}[\rho, \mathbf{j}_p]. \quad (1)$$

We are using Hartree atomic units throughout this paper and have used the Coulomb gauge for the external vector potential ($\nabla \cdot \mathbf{A} = 0$). In the above expression, the external scalar potential v_{nuc} is the electrostatic potential of the nuclei and the external vector potential $\mathbf{A}(\mathbf{r})$ corresponds to the magnetic field. The total energy functional contains terms for the noninteracting kinetic energy, the electron-nuclei attraction, the interaction of the current and of the electron density with the external vector potential, the Coulomb repulsion of the electrons, and the exchange-correlation energy, which now also depends on the current.

The noninteracting kinetic energy $T_s[\rho, \mathbf{j}_p]$ is the kinetic energy of a reference system of noninteracting electrons having the same electron density ρ and paramagnetic current \mathbf{j}_p as the interacting system. For such a system, the wave function is given by one single Slater determinant. The electron density is then given by

$$\rho(\mathbf{r}) = 2 \sum_{i=1}^N \phi_i^*(\mathbf{r})\phi_i(\mathbf{r}), \quad (2)$$

and the paramagnetic current is given by

$$\mathbf{j}_p(\mathbf{r}) = i \sum_{i=1}^N \{ \phi_i^*(\mathbf{r}) \nabla \phi_i(\mathbf{r}) - \phi_i(\mathbf{r}) \nabla \phi_i^*(\mathbf{r}) \}. \quad (3)$$

In this definition of the paramagnetic current the negative unit charge of the electron and the double occupation of the orbitals have been included.

Minimization of the total energy functional with respect to the the Kohn-Sham (KS) orbitals $\{\phi_i\}$ of this noninteracting reference system under the constraint that the KS orbitals are orthonormal leads to KS equations for the determination of the KS orbitals $\{\phi_i\}$,

$$\left[\frac{1}{2}(-i \nabla + \mathbf{A}(\mathbf{r}))^2 + \frac{i}{2}\mathbf{A}_{\text{xc}}(\mathbf{r}) \nabla + v_{\text{eff}}^{\text{KS}}[\rho](\mathbf{r}) \right] \phi_i(\mathbf{r}) = \epsilon_i \phi_i(\mathbf{r}). \quad (4)$$

The KS effective potential $v_{\text{eff}}^{\text{KS}}[\rho]$ contains the usual terms of the nuclear potential, the Coulomb potential of the electrons,

and the exchange-correlation potential. In addition, $\mathbf{A}_{xc}(\mathbf{r}) = \delta E_{xc}[\rho, \mathbf{j}_p] / \delta \mathbf{j}_p(\mathbf{r})$ enters these equations because of the current dependence of the exchange-correlation functional. It can be shown³⁵ that these one-electron equations are gauge invariant and that the total current $\mathbf{j}(\mathbf{r}) = \mathbf{j}_p(\mathbf{r}) - \rho(\mathbf{r})\mathbf{A}(\mathbf{r})$ obtained from it satisfies the continuity equation

$$\nabla \cdot \mathbf{j}(\mathbf{r}) + \frac{\partial \rho(\mathbf{r})}{\partial t} = 0. \quad (5)$$

For the calculation of NMR parameters, the current dependence of the exchange-correlation functional is usually neglected. This approximation is often referred to as ‘‘uncoupled DFT.’’ In this case, the KS equations for systems in a magnetic field reduce to

$$\left[\frac{1}{2}(-i\nabla + \mathbf{A}(\mathbf{r}))^2 + v_{\text{eff}}^{\text{KS}}[\rho](\mathbf{r}) \right] \phi_i(\mathbf{r}) = \epsilon_i \phi_i(\mathbf{r}). \quad (6)$$

These equations can also be obtained from the usual KS equations by substitution of the momentum operator $\hat{p} = -i\nabla$ with $\hat{p} + \mathbf{A}(\mathbf{r})$.

B. Nonrelativistic DFT calculation of NMR shieldings

The NMR shielding tensor can be expressed in terms of the first-order current induced by a homogeneous external magnetic field, which is probed by the nuclear magnetic moment of the nucleus in question, as³⁷

$$\sigma_{st} = -\frac{1}{c^2} \int \left[\frac{(\mathbf{r} - \mathbf{R}_{\text{nuc}}) \times \mathbf{j}^{B_t}(\mathbf{r})}{|\mathbf{r} - \mathbf{R}_{\text{nuc}}|^3} \right]_s d\mathbf{r}. \quad (7)$$

In this expression, the subscripts s and t refer to the individual Cartesian components, \mathbf{R}_{nuc} is the position of the NMR nucleus, and the first-order induced current is given by $\mathbf{j}^{B_t}(\mathbf{r}) = \partial \mathbf{j}(\mathbf{r}) / \partial B_t$, where the derivative is taken with respect to the Cartesian components of the external magnetic field \mathbf{B} .

As in the previous section, the induced current can be split up into a paramagnetic and a diamagnetic part,

$$\mathbf{j}^{B_t}(\mathbf{r}) = \mathbf{j}_p^{B_t}(\mathbf{r}) - \rho(\mathbf{r}) \frac{\partial \mathbf{A}(\mathbf{r})}{\partial B_t}. \quad (8)$$

With this decomposition, the shielding tensor can then also be written as a sum of a diamagnetic and a paramagnetic part,

$$\sigma_{st} = \sigma_{st}^D + \sigma_{st}^P. \quad (9)$$

The diamagnetic part of the shielding tensor is given by

$$\begin{aligned} \sigma_{st}^D &= \frac{1}{c^2} \int \left[\frac{(\mathbf{r} - \mathbf{R}_{\text{nuc}}) \times \rho(\mathbf{r})(\partial \mathbf{A}(\mathbf{r}) / \partial B_t)}{|\mathbf{r} - \mathbf{R}_{\text{nuc}}|^3} \right]_s d\mathbf{r} \\ &= \int h_{st}^{11} \rho(\mathbf{r}) d\mathbf{r}, \end{aligned} \quad (10)$$

with the diamagnetic shielding operator

$$h_{st}^{11} = \frac{1}{2} \frac{\mathbf{r} \cdot (\mathbf{r} - \mathbf{R}_{\text{nuc}}) \delta_{st} - r_s (\mathbf{r} - \mathbf{R}_{\text{nuc}})_t}{|\mathbf{r} - \mathbf{R}_{\text{nuc}}|^3}. \quad (11)$$

(We have followed the usual convention of specifying the order of the perturbation operator in the external magnetic

field as superscripts.) The diamagnetic part only depends on the unperturbed electron density and does not require the knowledge of the perturbed orbitals.

The paramagnetic part of the shielding tensor is given by

$$\sigma_{st}^P = -\frac{1}{c^2} \int \left[\frac{(\mathbf{r} - \mathbf{R}_{\text{nuc}}) \times \mathbf{j}_p^{B_t}(\mathbf{r})}{|\mathbf{r} - \mathbf{R}_{\text{nuc}}|^3} \right]_s d\mathbf{r} \quad (12)$$

and requires the knowledge of the first-order induced paramagnetic current $\mathbf{j}_p^{B_t}$, which can be determined from the response of the KS orbitals to a homogeneous external magnetic field. As described in the previous section, CDFT has to be used to describe systems in magnetic fields and in the approximation of uncoupled DFT, i.e., neglecting the current dependence of the exchange-correlation functional, the KS equations in the presence of a magnetic field are given by Eq. (6). To first order in the magnetic field strength, the perturbation that is introduced in these equations by a homogeneous external magnetic field is given by

$$\mathbf{h}^{10} = -\frac{i}{2} (\mathbf{r} \times \nabla). \quad (13)$$

This perturbation operator is purely imaginary, which implies that the first-order perturbed orbitals will also be purely imaginary and that the first-order change in the electron density vanishes.³⁸

Choosing the unperturbed KS orbitals as real so that the first-order perturbed orbitals are purely imaginary, the first-order induced paramagnetic current can be expressed in terms of the KS orbitals as

$$\mathbf{j}_p^{B_t}(\mathbf{r}) = 2i \sum_{i=1}^N \{ \phi_i^{(0)}(\mathbf{r}) \nabla \phi_i^{B_t}(\mathbf{r}) - \phi_i^{B_t}(\mathbf{r}) \nabla \phi_i^{(0)}(\mathbf{r}) \}, \quad (14)$$

where the superscript (0) is used to refer to the KS orbitals of the unperturbed system and the first-order perturbed orbitals $\phi_i^{B_t}(\mathbf{r}) = \partial \phi_i(\mathbf{r}) / \partial B_t$ describe the response of the KS orbitals to a homogeneous external magnetic field.

The first-order perturbed orbitals are usually determined by expanding them in terms of the canonical KS orbitals of the unperturbed system as

$$\phi_i^{B_t}(\mathbf{r}) = \sum_j u_{ij,t} \phi_j^{(0)}(\mathbf{r}), \quad (15)$$

where the coefficients $u_{ij,t}$ can easily be determined from

$$u_{ij,t} = -\frac{\langle \phi_i^{(0)} | h_t^{10} | \phi_j^{(0)} \rangle}{\epsilon_i - \epsilon_j}. \quad (16)$$

In practical applications with atom-centered basis functions, it is necessary to ensure the gauge invariance of the above formulation. It is well known that fast basis set convergence can be achieved by employing gauge-including atomic orbitals (GIAOs),³⁹ i.e., by including a magnetic-field-dependent phase factor in the basis functions. This leads to additional terms in the expressions for both the diamagnetic and the paramagnetic shielding.³⁷ For reasons of simplicity, we will not mention these additional terms in the following, they are, however, included in the implementation that is used.

C. Frozen-density embedding for systems in external magnetic fields

In the FDE formalism within DFT,^{18,19} the total electron density $\rho_{\text{tot}}(\mathbf{r})$ is split up into two components, $\rho^{(I)}(\mathbf{r})$ and $\rho^{(II)}(\mathbf{r})$, which add up to the total electron density,

$$\rho^{(\text{tot})}(\mathbf{r}) = \rho^{(I)}(\mathbf{r}) + \rho^{(II)}(\mathbf{r}). \quad (17)$$

Both $\rho^{(I)}(\mathbf{r})$ and $\rho^{(II)}(\mathbf{r})$ can then be determined separately from a set of one-electron equations in which the effect of the density in the other subsystem is represented in terms of an effective embedding potential.

To extend the FDE formalism to systems in magnetic fields, it is not sufficient to use only the electron density as a basic variable, since the energy is now also a functional of

the paramagnetic current. Therefore, we make the same ansatz and split the paramagnetic current into contributions from the two separate subsystems,

$$\mathbf{j}_p^{(\text{tot})}(\mathbf{r}) = \mathbf{j}_p^{(I)}(\mathbf{r}) + \mathbf{j}_p^{(II)}(\mathbf{r}). \quad (18)$$

With these definitions, also the total current is given as the sum of the currents of the two subsystems, $\mathbf{j}^{(\text{tot})}(\mathbf{r}) = \mathbf{j}^{(I)}(\mathbf{r}) + \mathbf{j}^{(II)}(\mathbf{r})$. Furthermore, it has to be noticed that if the continuity equation [Eq. (5)] is satisfied for each of the two subsystems individually, it is also satisfied for the total system and the above partitioning of the electron density and of the paramagnetic current are, therefore, justified in this case.

With this partitioning of the electron density and of the paramagnetic current, the total energy functional for systems in magnetic fields of Eq. (1) can be formulated as a bifunctional in terms of the electron densities and paramagnetic currents of the two subsystems,

$$\begin{aligned} E[\rho^{(I)}, \mathbf{j}_p^{(I)}, \rho^{(II)}, \mathbf{j}_p^{(II)}] &= T_s[\rho^{(I)}, \mathbf{j}_p^{(I)}] + T_s[\rho^{(II)}, \mathbf{j}_p^{(II)}] + T_s^{\text{nadd}}[\rho^{(I)}, \mathbf{j}_p^{(I)}, \rho^{(II)}, \mathbf{j}_p^{(II)}] + \int (\rho^{(I)}(\mathbf{r}) + \rho^{(II)}(\mathbf{r}))(v_{\text{nuc}}^{(I)}(\mathbf{r}) + v_{\text{nuc}}^{(II)}(\mathbf{r}))d\mathbf{r} \\ &+ \int \frac{(\rho^{(I)}(\mathbf{r}) + \rho^{(II)}(\mathbf{r}))(\rho^{(I)}(\mathbf{r}') + \rho^{(II)}(\mathbf{r}'))}{|\mathbf{r} - \mathbf{r}'|} d\mathbf{r}d\mathbf{r}' - \int (\mathbf{j}_p^{(I)}(\mathbf{r}) + \mathbf{j}_p^{(II)}(\mathbf{r}))\mathbf{A}(\mathbf{r})d\mathbf{r} \\ &+ \frac{1}{2} \int (\rho^{(I)}(\mathbf{r}) + \rho^{(II)}(\mathbf{r}))\mathbf{A}^2(\mathbf{r})d\mathbf{r} + E_{\text{xc}}[\rho^{(I)} + \rho^{(II)}, \mathbf{j}_p^{(I)} + \mathbf{j}_p^{(II)}], \end{aligned} \quad (19)$$

where the nonadditive kinetic-energy functional T_s^{nadd} is defined as

$$\begin{aligned} T_s^{\text{nadd}}[\rho^{(I)}, \mathbf{j}_p^{(I)}, \rho^{(II)}, \mathbf{j}_p^{(II)}] &= T_s[\rho^{(I)} + \rho^{(II)}, \mathbf{j}_p^{(I)} + \mathbf{j}_p^{(II)}] \\ &- T_s[\rho^{(I)}, \mathbf{j}_p^{(I)}] - T_s[\rho^{(II)}, \mathbf{j}_p^{(II)}]. \end{aligned} \quad (20)$$

If the densities and currents are represented using the KS orbitals of the individual subsystems, it is possible to calculate the noninteracting kinetic energy $T_s[\rho^{(I,II)}, \mathbf{j}_p^{(I,II)}]$ of the separate subsystems directly. However, with the partitioning of the electron density and current into the contributions of the two subsystems, the canonical KS orbitals of the total system are in general not available, so that the noninteracting kinetic energy $T_s[\rho^{(\text{tot})}, \mathbf{j}_p^{(\text{tot})}]$ of the total system cannot be calculated in this way. For this reason, in practical applications of the FDE scheme an appropriate orbital-independent approximation of T_s^{nadd} has to be applied.

The total energy bifunctional of Eq. (19) does not contain a current-current interaction between the currents in systems I and II. This magnetic interaction is not present in the nonrelativistic limit of electrodynamics,³⁸ where the electrons only interact via the Coulomb interaction, i.e., a magnetic electron-electron interaction is not included.

For a given electron density and paramagnetic current in subsystem II, the KS orbitals of subsystem I, $\{\phi_i^{(I)}\}$, can now be obtained by minimizing $\mathbf{E}[\rho^{(I)}, \mathbf{j}_p^{(I)}, \rho^{(II)}, \mathbf{j}_p^{(II)}]$ with respect

to the KS orbitals of subsystem I, under the constraint that these orbitals are orthonormal. This leads to a set of one-electron equations for the KS orbitals $\{\phi_i^{(I)}\}$,

$$\begin{aligned} &\left[\frac{1}{2}(-i\nabla + \mathbf{A}(\mathbf{r}))^2 + v_{\text{eff}}^{\text{KSCED}}[\rho^{(I)}, \rho^{(II)}](\mathbf{r}) \right. \\ &\quad \left. + i \frac{\delta T_s^{\text{nadd}}[\rho^{(I)}, \mathbf{j}_p^{(I)}, \rho^{(II)}, \mathbf{j}_p^{(II)}]}{\delta \mathbf{j}_p^{(I)}(\mathbf{r})} \nabla \right. \\ &\quad \left. + i \frac{\delta E_{\text{xc}}[\rho^{(I)} + \rho^{(II)}, \mathbf{j}_p^{(I)} + \mathbf{j}_p^{(II)}]}{\delta \mathbf{j}_p^{(I)}(\mathbf{r})} \nabla \right] \phi_i^{(I)}(\mathbf{r}) = \epsilon_i \phi_i^{(I)}(\mathbf{r}). \end{aligned} \quad (21)$$

These equations will, as in the case without magnetic fields, be referred to as Kohn-Sham equations with constrained electron density (KSCED). The KSCED effective potential in the above equations is given by

$$v_{\text{eff}}^{\text{KSCED}}[\rho^{(I)}, \rho^{(II)}](\mathbf{r}) = v_{\text{eff}}^{\text{KS}}[\rho^{(I)}](\mathbf{r}) + v_{\text{eff}}^{\text{emb}}[\rho^{(I)}, \rho^{(II)}](\mathbf{r}), \quad (22)$$

where $v_{\text{eff}}^{\text{KS}}[\rho^{(I)}](\mathbf{r})$ is the KS effective potential of the isolated subsystem I containing the usual terms of the nuclear potential, Coulomb potential of the electrons, and the exchange-correlation potential. The effective embedding potential $v_{\text{eff}}^{\text{emb}}[\rho^{(I)}, \rho^{(II)}](\mathbf{r})$ describes the interaction of the subsystem I with the frozen density of subsystem II and reads

$$v_{\text{eff}}^{\text{emb}}[\rho^{(\text{I})}, \rho^{(\text{II})}](\mathbf{r}) = v_{\text{II}}^{\text{nuc}}(\mathbf{r}) + \int \frac{\rho^{(\text{II})}(\mathbf{r}')}{|\mathbf{r} - \mathbf{r}'|} d\mathbf{r}' + \left. \frac{\delta E_{\text{xc}}[\rho]}{\delta \rho} \right|_{\rho=\rho^{(\text{tot})}(\mathbf{r})} - \left. \frac{\delta E_{\text{xc}}[\rho]}{\delta \rho} \right|_{\rho=\rho^{(\text{I})}(\mathbf{r})} + \frac{\delta T_s^{\text{nadd}}[\rho^{(\text{I})}, \rho^{(\text{II})}]}{\delta \rho^{(\text{I})}(\mathbf{r})}. \quad (23)$$

The KS orbitals of subsystem I can then be obtained by solving the KSCED equations self-consistently.

If the assumption that $\rho^{(\text{tot})} - \rho^{(\text{II})}$ is positive and v_s -representable⁴⁰ and that $\mathbf{j}_p^{(\text{tot})} - \mathbf{j}_p^{(\text{II})}$ is v_s -representable is fulfilled, the solution of Eq. (21) will—in the case that the exact nonadditive kinetic-energy functional would be used—yield the same total electron density and total current as the solution of Eq. (4), i.e., as the corresponding supermolecular KS-DFT calculation (using the same approximation for the exchange-correlation functional). If the initial assumptions are not satisfied, Eq. (21) can be solved in “freeze-and-thaw” cycles by exchanging the role of the frozen and nonfrozen systems, i.e., by solving two coupled sets of KSCED equations for subsystems I and II.

Usually in the calculation of NMR parameters the current dependence of the exchange-correlation functional is neglected. In this case, the corresponding term drops out of the KSCED equations. However, in the case that the exact nonadditive kinetic-energy functional would be used, the solution of the KSCED equations will still yield the same solution as the supermolecular KS-DFT calculation in which the same approximation is made.

In practical applications of the FDE formalism, approximations have to be used for the nonadditive kinetic-energy functional. The approximations that are available for the nonadditive kinetic-energy functional⁴¹ do not include a current dependence. For the calculation of NMR parameters it will, therefore, be the first choice to apply these approximations and to neglect the current dependence. It can be expected that for weakly interacting systems, where the available approximations are applicable, the error introduced by the neglect of the current dependence is smaller than the intrinsic error of the approximate functionals. However, the validity of this assumption has to be assessed in test calculations of NMR parameters.

If the current dependence both of the nonadditive kinetic-energy functional and of the exchange-correlation functional is neglected, the KSCED equations reduce to

$$\left[\frac{1}{2}(-i\nabla + \mathbf{A}(\mathbf{r}))^2 + v_{\text{eff}}^{\text{KSCED}}[\rho^{(\text{I})}, \rho^{(\text{II})}](\mathbf{r}) \right] \phi_i^{(\text{I})}(\mathbf{r}) = \epsilon_i \phi_i^{(\text{I})}(\mathbf{r}). \quad (24)$$

The absence of a magnetic interaction between the currents in the two subsystems and the neglect of the current dependence of T_s^{nadd} and of E_{xc} have the consequence that the KSCED equations for subsystems I and II are not coupled via the current. This means that calculations on the nonfrozen subsystem can be carried out without knowledge of the induced current in the frozen subsystem.

Finally, it is important to note that the electron density and current that are given by the KS orbitals obtained from the KSCED equations will satisfy the continuity equation [Eq. (5)], because the KSCED equations are of the same form as the KS equations of CDFT.

D. Calculation of NMR shieldings with frozen-density embedding

The FDE formalism described in the previous section is now applied to the calculation of NMR shielding tensors by decomposing the first-order current induced by an external homogeneous magnetic field into the contributions of the two individual subsystems,

$$\mathbf{j}^{B_i} = \mathbf{j}^{(\text{I})B_i} + \mathbf{j}^{(\text{II})B_i}. \quad (25)$$

With this decomposition, also the shielding tensor [Eq. (7)] separates into contributions of the two subsystems,

$$\sigma_{st} = \sigma_{st}^{(\text{I})} + \sigma_{st}^{(\text{II})}, \quad (26)$$

where

$$\sigma_{st}^{(n)} = -\frac{1}{c^2} \int \left[\frac{(\mathbf{r} - \mathbf{R}_{\text{nuc}}) \times \mathbf{j}^{(n)B_i}(\mathbf{r})}{|\mathbf{r} - \mathbf{R}_{\text{nuc}}|^3} \right]_s d\mathbf{r} \quad (n = \text{I, II}). \quad (27)$$

As before, these can again be split up into diamagnetic and paramagnetic contributions.

These contributions to the shielding tensor are determined separately for the individual subsystems. The starting point is the determination of the ground-state electron density of the two subsystems by solving the KSCED equations for both fragments in freeze-and-thaw cycles. The diamagnetic shielding can then be evaluated directly, since it only depends on the unperturbed electron densities,

$$\sigma_{st}^D = \sigma_{st}^{D,(\text{I})} + \sigma_{st}^{D,(\text{II})}, \quad (28)$$

with

$$\sigma_{st}^{D,(n)} = \int h_{st}^{11} \rho^{(n)}(\mathbf{r}) d\mathbf{r} \quad (n = \text{I, II}). \quad (29)$$

The calculation of the paramagnetic shielding requires the determination of the first-order current that is induced by a homogeneous external magnetic field in each subsystem. For the evaluation of the induced current in one of the subsystems, the induced current in the frozen system is not needed because there is no dependence on the current in the frozen subsystem in Eq. (24) and because the homogeneous external magnetic field does not induce a first-order change in the electron density (see Sec. II B), i.e., the external magnetic field does not induce any coupling between the two subsystems. Therefore, the first-order perturbed orbitals and thus the induced paramagnetic current can be determined separately for the subsystems by using Eq. (16) and it is not necessary to determine the induced current in freeze-and-thaw cycles. Within the FDE formalism, the paramagnetic shielding can thus simply be calculated by adding the contributions of the individual subsystems,

$$\sigma_{st}^P = \sigma_{st}^{P,(I)} + \sigma_{st}^{P,(II)}, \quad (30)$$

with

$$\sigma_{st}^{P,(n)} = -\frac{1}{c^2} \int \left[\frac{(\mathbf{r} - \mathbf{R}_{\text{nuc}}) \times \mathbf{j}_p^{(n)Bt}(\mathbf{r})}{|\mathbf{r} - \mathbf{R}_{\text{nuc}}|^3} \right]_s d\mathbf{r} \quad (n = I, II). \quad (31)$$

In the calculation of the NMR shielding of one subsystem, no additional contributions arise due to the other subsystem, i.e., all the effects of the other (frozen) subsystem are included already in the effective embedding potential that is used in the determination of the ground-state electron density and KS orbitals.

Two approximations are made in the theory presented above. First, the approximation of uncoupled DFT is employed, i.e., the current dependence of the exchange-correlation functional is neglected. This approximation is consistently made both in supermolecular DFT calculations and in FDE calculations of NMR shieldings. Second, the current dependence of the nonadditive kinetic-energy functional is also neglected. It can be expected that this approximation is only valid if the interaction between the two subsystems is sufficiently weak and that in the case of stronger interactions, such as chemical bonds, between the subsystems, it will not be possible to neglect the current dependence of the nonadditive kinetic-energy functional anymore. The validity of this approximation will therefore depend on choosing an appropriate partitioning into subsystems. However, the same restrictions apply for the available approximate functionals for the nonadditive kinetic energy.

In the calculation of NMR shieldings, the induced current is only probed by the nuclear spin of the NMR nucleus in question [see Eq. (7)], so that the most important contributions to the shielding tensor are due to the induced current in the vicinity of the NMR nucleus. The subsystem-based formulation of the calculation of NMR shieldings presented above has the advantage that it makes it possible to exploit this near sightedness of the NMR shielding very easily. The main contribution to the NMR shielding and to chemical shifts is the contribution of the subsystem that contains the NMR nucleus. In many cases, it will be possible to neglect the contribution of the other subsystem to the NMR shielding, i.e., the effect of the other subsystem is only included in the calculation of the ground-state density and KS orbitals. It is also possible to construct the electron density of an environment using further approximations, for instance by using a sum-of-fragments density, or by applying freeze-and-thaw cycles only for parts of the system that are close to the subsystem of interest.^{22,20}

III. COMPUTATIONAL DETAILS

All density-functional calculations were performed using the Amsterdam density-functional (ADF) package.^{42,43} The FDE scheme of Wesolowski and Warshel¹⁸ has been implemented in the most recent version of ADF using an efficient numerical integration scheme.²³ For the nonadditive kinetic-energy component of the embedding potential we chose to employ, based on previous results of Wesolowski

et al.,^{41,44,45} the PW91k kinetic-energy functional.⁴⁶

The calculations of NMR shieldings were performed using the NMR program of Schreckenbach and Ziegler that is part of the ADF package,⁴⁷ which calculates the shielding tensor using GIAOs.³⁹ The calculation of NMR shieldings using the FDE scheme does not require major modifications of the program that is used for the calculation of the shielding. It only has to be ensured that the electron density and KS orbitals obtained from a FDE calculation can be used and that the effective embedding potential is included in the total KS potential that is needed in the NMR calculation. In addition, the calculation of the contribution of the frozen subsystem to the shielding requires the possibility to calculate the shielding tensor at an arbitrary position [nucleus-independent chemical shifts (NICs)], which we implemented in the NMR program of ADF for this work.

We have used two different approximations for the exchange-correlation potential, the generalized-gradient approximation (GGA) functional BP86, consisting of the exchange functional by Becke⁴⁸ and the correlation functional by Perdew,⁴⁹ and the “statistical averaging of molecular orbital potential” (SAOP),^{50–52} which has been shown to improve the description of NMR chemical shifts significantly with respect to GGA functionals.⁵³ In the FDE calculations using the orbital-dependent SAOP potential, the exchange-correlation component of the effective embedding potential was approximated using the Becke-Perdew-Wang (BPW91) exchange-correlation functional.^{48,54}

We have used the TZ2P basis set from the ADF basis set library, which is of triple- ζ quality and contains two sets of polarization functions, and the ZORA-QZ4P basis set, which is of quadruple- ζ quality and contains four sets of polarization functions.

IV. RESULTS AND DISCUSSION

To assess the quality of chemical shifts calculated using the FDE formalism we have performed test calculations on small systems. The accuracy of the FDE calculations can be tested by comparing them to supermolecular KS-DFT calculations using the same approximation for the exchange-correlation functional.⁵⁵ In the limit that the exact (current-dependent) nonadditive kinetic-energy functional is used, both methods should yield identical results.

As a test application, we investigate the effect of different solvents on the nitrogen shielding in acetonitrile, CH₃CN. The nitrogen shielding is known to be very sensitive to environment effects, and the nitrogen shielding in acetonitrile has been used as a model system for studying environment effects on NMR chemical shifts in earlier studies.^{15,56}

As model systems for these solvent effects, we have used small clusters consisting of acetonitrile and one solvent molecule. As solvents we have investigated water, chloroform, cyclohexane, and benzene. This simple cluster model will certainly not be able to give a realistic description of all solvent effects on the nitrogen chemical shifts. A more realistic description would require the inclusion of a much larger number of solvent molecules and would also require the in-

clusion of the dynamics in solution. However, this is not the purpose of this study, as we only want to assess the accuracy of the FDE calculation by comparing to supermolecular KS-DFT calculations.

There are different approximations involved in the FDE scheme that can lead to differences with respect to supermolecular KS-DFT calculations. First, approximations have to be used for the nonadditive kinetic-energy functional, and for the calculation of NMR chemical shifts the current dependence of the nonadditive kinetic energy is neglected. Second, in calculations using orbital-dependent approximations to the exchange-correlation potential such as SAOP, one furthermore encounters the complication that the supermolecular exchange-correlation potential is constructed in terms of a set of supermolecular orbitals. This potential cannot be reconstructed in a KSCED calculation since only the subsystem orbitals are available. This makes it necessary to choose a non-orbital-dependent form for the nonadditive exchange-correlation contribution to the effective embedding potential, introducing an additional inconsistency relative to the supermolecular calculation.⁵⁵ This is not the case with a GGA potential such as BP86, because then the same approximation can be used for the exchange-correlation potential in the subsystems and for the nonadditive exchange-correlation contribution to the embedding potential.

A third origin of differences with respect to the supermolecular calculation is the finite basis set that is used.⁴¹ The most obvious choice for the basis set in the FDE calculations is to use only basis functions that are centered on the atoms in the considered subsystem to expand the corresponding density. Calculations using this monomolecular basis set expansion will be labeled FDE(*m*). However, this choice of the basis functions introduces an additional source of differences to the supermolecular calculation. In the expansion of the total electron density the products of basis functions centered at atoms in different subsystems are neglected. Furthermore, since the total number of electrons in both subsystems is fixed, a charge transfer between the two subsystems is not possible. These problems are both removed if the full supermolecular basis set is used to expand the density of both subsystems. Calculations using this supermolecular basis set expansion will be labeled FDE(*s*).

In addition, further approximations can be applied in the construction of the electron density of the solvent. Instead of obtaining the electron density of the two subsystems using freeze-and-thaw cycles, the electron density of the solvent can be obtained from a gas-phase calculation (i.e., the electron density of the isolated solvent molecule is used). Such a gas-phase density can be improved by applying one single freeze-and-thaw cycle (i.e., the gas-phase density is polarized). In the following, we will indicate the number of freeze-and-thaw cycles that have been applied. Calculations using the frozen gas-phase density of the solvent will be labeled FDE(*x*,0), calculations in which one single freeze-and-thaw cycle was applied will be labeled FDE(*x*,1), and calculations in which freeze-and-thaw cycles were applied until the NMR shielding was converged will be labeled FDE(*x*,∞), where *x*=*s*,*m* indicate the basis set expansion that was used.

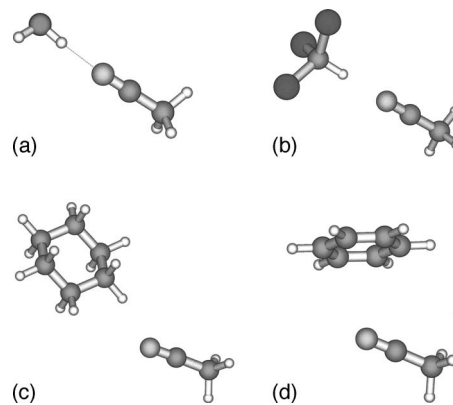


FIG. 1. Structures of the acetonitrile-solvent clusters used in the calculations: (a) acetonitrile-water, (b) acetonitrile-chloroform, (c) acetonitrile-cyclohexane, and (d) acetonitrile-benzene.

Finally, in the FDE calculation of NMR shieldings the contribution of the induced current in the solvent subsystem to the shielding has to be included to be consistent with the supermolecular KS-DFT calculation. As we will see, it is possible to neglect this additional contribution in many cases.

The structures of the acetonitrile-solvent clusters that were used in the calculations are shown in Fig. 1. These structures have been obtained from geometry optimizations using the BP86 exchange-correlation functional in combination with a TZ2P basis set. They have been confirmed to represent local minima on the potential energy surface, but they do not represent global minima.

In the following we will investigate the solvent shifts on the isotropic shielding of the nitrogen nucleus in acetonitrile, which are defined as

$$\Delta\sigma = \sigma_{\text{cluster}} - \sigma_{\text{acetonitrile}}, \quad (32)$$

where σ_{cluster} denotes the isotropic shielding as calculated for the acetonitrile-solvent cluster (either using a supermolecular KS-DFT calculation or a FDE calculation) and $\sigma_{\text{acetonitrile}}$ denotes the isotropic shielding calculated for the isolated acetonitrile molecule. For the calculations on the isolated acetonitrile molecule, the same geometry as in the acetonitrile-solvent cluster is used, i.e., the change of the acetonitrile geometry due to the presence of the solvent molecule is not included in the solvent shift. This geometric effect is the same for both supermolecular KS-DFT calculations and for the FDE calculations, since the same geometries are used in both calculations.

For each acetonitrile-solvent cluster considered, the solvent shifts for calculations using the same exchange-correlation functional and basis set are reported with respect to the same isolated acetonitrile calculation, i.e., all differences between supermolecular KS-DFT calculations and FDE calculations, as well as differences between FDE calculations employing different additional approximations, are visible in the reported solvent shifts.

A. Acetonitrile-water

First, we investigate the acetonitrile-water cluster as a model for the effects of a water solution on the nitrogen

TABLE I. Solvent shift of the nitrogen NMR shielding in the acetonitrile-water cluster relative to isolated acetonitrile, calculated using supermolecular KS-DFT calculations and FDE calculations. See text for details.

	BP86		SAOP	
	TZ2P	QZ4P	TZ2P	QZ4P
Supermolecule	15.89	15.05	17.73	16.99
FDE($m, 0$)	12.57	12.04	12.18	11.89
FDE($m, 1$)	16.49	16.41	15.58	15.63
FDE(m, ∞)	16.64	16.64	15.70	15.79
FDE(s, ∞)	17.16	16.44	15.82	15.40

chemical shift in acetonitrile. Due to the formation of a hydrogen bond between the solvent water molecule and the nitrogen atom of the acetonitrile, which is also the NMR nucleus under investigation, a large solvent shift can be expected. The results obtained for the acetonitrile-water cluster are summarized in Table I.

As expected, the supermolecular KS-DFT calculations show a large solvent shift on the nitrogen shielding in acetonitrile of 15.05 ppm using the GGA functional BP86 and of 16.99 ppm using the SAOP potential. With both functionals, the change in the solvent shift when going from the TZ2P to the larger QZ4P basis set is smaller than 1 ppm, so that with respect to the basis set the solvent shifts can be considered as converged within this accuracy. It should be noted that this is not the case for the absolute shieldings, which still show a strong basis set dependence due to the addition of more tight basis functions. In the calculations using the BP86 functional, the absolute nitrogen shielding in acetonitrile changes from -24.71 to -31.19 ppm when going from the TZ2P to the QZ4P basis set, in the calculations using SAOP it changes from -17.76 to 22.17 ppm.

Already using the most simple embedding method, labeled FDE($m, 0$) in the table, in which the frozen electron density is taken from an isolated water molecule, the largest part of the solvent shift is recovered, and the solvent shift calculated for the supermolecule is underestimated by only approximately 3 ppm for the BP86 calculations and approximately 5 ppm for the SAOP calculations. If the frozen density is polarized in one single freeze-and-thaw cycle [FDE($m, 1$)], the solvent shifts agree very well with the supermolecular calculation. With the BP86 functional, the differences are for both basis sets smaller than 1.4 ppm. In the calculations using SAOP, where an additional approximation has to be made in the nonadditive kinetic-energy functional, the differences are slightly larger, but still for both basis sets smaller than 2.3 ppm. These differences are small compared to the range of the nitrogen shielding scale of about 600 ppm for organic molecules.

Applying freeze-and-thaw cycles until the NMR shieldings are converged to the accuracy reported here does not change the solvent shifts significantly. In all cases, convergence is achieved after at most three full freeze-and-thaw cycles. The inclusion of basis functions located on the frozen subsystem does not change the solvent shifts significantly either.

One interesting finding is that the difference between the

TABLE II. Solvent shift of the nitrogen NMR shielding in the acetonitrile-chloroform cluster relative to isolated acetonitrile, calculated using supermolecular KS-DFT calculations and FDE calculations. See text for details.

	BP86		SAOP	
	TZ2P	QZ4P	TZ2P	QZ4P
Supermolecule	12.91	12.24	14.11	13.97
FDE($m, 0$)	10.35	9.87	9.04	8.52
FDE($m, 1$)	14.76	14.81	13.07	12.97
FDE(m, ∞)	14.96	15.09	13.23	13.23
FDE(s, ∞)	15.22	14.82	13.04	12.86

results obtained with the different basis sets is much smaller in the FDE(m, ∞) calculations than in the FDE(s, ∞) and in the supermolecular calculations. This can be explained by the absence of basis set superposition error (BSSE) in the case of the FDE(m) calculations. In these calculations BSSE is explicitly excluded because no basis functions on the frozen fragment are included. However, the FDE(s, ∞) calculations and not the BSSE-free FDE(m, ∞) calculations have to be compared to the supermolecular calculations, since both will consistently include a BSSE of approximately the same size. Even though the basis set convergence in the BSSE-free FDE(m, ∞) calculations is faster, the small differences between the FDE(m, ∞) and the FDE(s, ∞) results, as well as the small differences between the results using the different basis sets, show that the BSSE is sufficiently small compared to other sources of errors.

The contribution of the induced current in the frozen water molecule to the shielding is in all FDE calculations smaller than 0.2 ppm and thus negligible and has not been included in the solvent shifts given in the table.

B. Acetonitrile-chloroform

As another example of a polar solvent we have looked at chloroform. The solvent shifts calculated for the acetonitrile-chloroform cluster are summarized in Table II.

The supermolecular KS-DFT calculations show a large solvent shift of the nitrogen shielding, but the shifts calculated with the QZ4P basis set of 12.91 and 13.97 ppm with BP86 and SAOP, respectively, are smaller than for the acetonitrile-water cluster because of the smaller polarity of the solvent molecule. As for water, the FDE($m, 0$) calculations are able to recover the largest part of this solvent shift, underestimating the shift calculated in the supermolecule. If the frozen density is allowed to be polarized, differences between FDE and the supermolecular calculation are reduced. In the calculations using the BP86 functional, the agreement is with both basis sets better than 2.6 ppm, with SAOP the differences are even below 1 ppm. However, as there is an additional approximation involved in the case of the SAOP calculations, this better agreement is probably due to a fortunate error cancellation between the nonadditive kinetic-energy functional and the nonadditive exchange-correlation functional.

As for the acetonitrile-water cluster, using additional freeze-and-thaw cycles and including basis functions on the frozen system does not change the solvent shifts signifi-

TABLE III. Solvent shift of the nitrogen NMR shielding in the acetonitrile-cyclohexane cluster relative to isolated acetonitrile, calculated using supermolecular KS-DFT calculations and FDE calculations. See text for details.

	BP86		SAOP	
	TZ2P	QZ4P	TZ2P	QZ4P
Supermolecule	0.39	0.32	2.88	2.45
FDE($m,0$)	0.07	0.29	-0.24	-0.06
FDE($m,1$)	2.21	2.77	1.70	2.13
FDE(m,∞)	2.27	2.85	1.74	2.19
FDE(s,∞)	2.50	2.51	1.63	1.71

cantly. Again the contribution of the induced current in the (frozen) chloroform molecule is smaller than 0.2 ppm.

C. Acetonitrile-cyclohexane

As an example of a nonpolar solvent we have investigated cyclohexane and the solvent shifts obtained for the acetonitrile-cyclohexane cluster are summarized in Table III.

As expected for the weak interaction between acetonitrile and the nonpolar cyclohexane, the solvent shift is very small. The calculations using the QZ4P basis set predict with the BP86 functional a solvent shift of 0.32 ppm and with SAOP a solvent shift of 2.24 ppm. In the FDE($m,0$) calculations the solvent shift is almost zero (smaller than 0.3 ppm) with both functionals. However, if one freeze-and-thaw cycle is applied for the solvent molecule the solvent shift increases by about 2 ppm. In the case of the BP86 functional, this leads to an overestimation of the supermolecular shift by ~ 2.5 ppm. With SAOP, the agreement with the supermolecular result is very good, but again this is probably due to a fortunate error cancellation.

Even though the absolute error is of the same size in the case of water and of chloroform, the relative error is unacceptably large if one is interested in accurate results for nonpolar solvents. As it is believed that the PW91k kinetic-energy functional that is used for the kinetic-energy component in the embedding potential is rather accurate for weakly interacting systems, this is quite surprising. It could be that the larger error in the calculation of NMR parameters is caused by the neglect of the current dependency of the nonadditive kinetic-energy functional. However, even with these large relative errors, the solvent shifts predicted by FDE are qualitatively correct and the absolute error is comparable to the differences between different approximations for the exchange-correlation functional.

Also for the acetonitrile-cyclohexane cluster, neither additional freeze-and-thaw cycles nor the inclusion of the basis functions of the frozen system changes the solvent shifts significantly. As expected the contribution of the induced current of the environment is below 0.2 ppm and is therefore neglected.

D. Acetonitrile-benzene

Finally, we have considered benzene as the prototypical nonpolar, aromatic solvent. For aromatic solvents, the contributions of the induced current in the solvent are expected to

TABLE IV. Solvent shift of the nitrogen NMR shielding in the acetonitrile-benzene cluster relative to isolated acetonitrile, calculated using supermolecular KS-DFT calculations and FDE calculations. The environment contribution of the induced current in the benzene molecule to the shielding is labeled "env." See text for details.

	BP86		SAOP	
	TZ2P	QZ4P	TZ2P	QZ4P
Supermolecule	-2.74	-0.29	0.69	2.42
FDE($m,0$)	-4.60	-2.53	-3.88	-2.10
FDE($m,1$)	-3.47	-1.20	-2.87	-0.95
FDE(m,∞)	-3.46	-1.18	-2.86	-0.97
FDE(s,∞)	-3.39	-1.04	-3.06	-1.10
env(m,∞)	+1.34	+1.37	+1.32	+1.39
FDE+env(m,∞)	-2.12	0.19	-1.54	0.42
FDE+env(s,∞)	-2.07	0.31	-1.76	0.24

be significant, because there are large currents induced in the aromatic solvent.^{57,58} These effects have also been explored experimentally and are known as aromatic solvent induced shifts (ASISs).⁵⁹ The solvent shifts calculated for the acetonitrile-benzene cluster are summarized in Table IV.

The supermolecular calculations using the BP86 functional predict a small negative solvent shift of -0.29 ppm with the QZ4P basis set for the acetonitrile-benzene cluster considered here. In contrast to that, the shift of 2.42 ppm predicted by the supermolecular calculations using the SAOP potential and the QZ4P basis set is also small, but positive. In addition, the results obtained using the TZ2P and the QZ4P basis set differ in both cases by about 2.0–2.5 ppm. This worse basis set convergence compared to the systems considered earlier can be attributed to the importance of diffuse basis functions in this weakly interacting system. Even though the supermolecular calculations do not provide a clear picture, it is still possible to compare the results obtained to the FDE calculations using the same functional and basis set.

As for the other systems, only one single freeze-and-thaw cycle is sufficient to converge the solvent shift to the required accuracy and also the inclusion of the basis functions of the frozen system is not important. When using the BP86 functional, the FDE($m,1$) calculations predict a solvent shift that is with the TZ2P basis set 0.73 ppm smaller and for the QZ4P basis set 0.91 ppm smaller than the solvent shift obtained from the supermolecular calculation. In the calculations using SAOP, the difference amounts to 3.56 ppm with the TZ2P basis set and 3.37 ppm with the QZ4P basis set. These differences found in the calculations using SAOP are larger than those found for the other systems.

The picture changes when the contribution of the induced current in the benzene molecule is included. This environment contribution, which can be calculated from a calculation of the NICS at the position of the nitrogen nucleus for the benzene molecule (using the electron density and KS orbitals obtained in the embedding calculation), is given in Table IV in the row labeled env(m,∞). It amounts to approximately 1.4 ppm and can therefore certainly not be neglected. If this contribution is included, the agreement be-

tween the FDE(m) calculations and the supermolecular calculations improves significantly. In the calculations using BP86, the differences are for both basis sets smaller than 0.7 ppm, for the calculations using SAOP they are smaller than 2.3 ppm.

V. CONCLUSIONS

In this paper, we have presented an extension of the frozen-density embedding (FDE) formalism to the calculation of NMR chemical shifts. This leads to a formulation of the nonrelativistic DFT calculation of NMR shieldings that is based on the partitioning of the system into several fragments, which are treated separately. For each fragment the ground-state density as well as the first-order current induced by a homogeneous external magnetic field are calculated separately and the effect of the other (frozen) fragments is included via an effective embedding potential. If the current dependence of the exchange-correlation functional and of the nonadditive kinetic-energy functional are neglected, this embedding potential does not depend on the induced current in the frozen fragment. This absence of a coupling via the current makes it possible to simply calculate the contributions of the individual fragments to the NMR shielding from their ground-state electron densities and KS orbitals.

The formalism presented is very well suited to exploit the near sightedness of the NMR shielding by applying additional approximations, e.g., by neglecting the induced current in fragments that are far away from the NMR nucleus and by using simplified ways of constructing the electron density of the fragments that do not contain the NMR nucleus.

Our test applications to small clusters of acetonitrile with different solvents show that the FDE scheme is able to reproduce the solvent shifts calculated in supermolecular KS-DFT calculations. The error of the FDE calculations with respect to the supermolecular calculations is about 2 ppm for the nitrogen shielding investigated here, which is about as large as the error of the currently available approximate exchange-correlation functionals. If the SAOP potential is used, the errors with respect to the supermolecular calculation are in most cases smaller, which is probably due to error cancellation.

Whereas absolute errors as large as 2 ppm are acceptable in the case of water and chloroform, where the frozen solvent molecule is very close to the NMR nucleus and even forms direct hydrogen bonds to the NMR nucleus, an error of this size is quite large in the case of weaker interactions, where the solvent shift is smaller. For these systems, improvements in the approximations to the nonadditive kinetic-energy functional might be needed to achieve more reliable results. If in future applications to larger systems a higher accuracy is required, it is possible to circumvent this problem by simply extending the nonfrozen fragment. This strategy has already been followed in earlier works.²³

The test calculations further show that for the systems studied here it is not necessary to include basis functions that are centered on the frozen fragments, making it possible to employ the computationally simpler FDE(m) scheme. How-

ever, it is in most cases required to include the polarization of the frozen solvent density by one single freeze-and-thaw cycle, especially if hydrogen bonds are present between solvent and solute. This is similar to what was found in earlier studies, where the FDE formalism was applied to modeling solvent effects on different other molecular properties.²⁰

In most cases it is possible to neglect the contribution of the induced current in the solvent molecule to the shielding, only for an aromatic solvent, where these induced currents are large, is this additional contribution significant, but even in this case it is possible to retain the separation of the total system into separate fragments. For a realistic modeling of the effects of an aromatic solvent on the NMR shielding of solute molecules, the contributions will become even more important, because these contributions of the currents induced in neighboring solvent molecules will add up to a large contribution of the aromatic environment.^{57,59}

For an application of the FDE scheme to a realistic modeling of solvent shift in NMR shieldings it will be necessary to use much larger solvent environments than in the test systems studied here, requiring also a proper sampling of a large number of solvent structures. This is feasible using the FDE scheme, as has been shown in earlier studies of solvent effects on different properties by Neugebauer *et al.*²²⁻²⁴ Its extension to the calculation of NMR chemical shifts presented in this paper and the good agreement between the FDE calculations and supermolecular DFT calculations we found for a number test systems make this kind of applications to large systems attractive. Furthermore, the possibility to describe the induced currents in the environment allows the applications of the FDE scheme to the calculation of NMR chemical shifts for systems in environments where these play an important role, such as aromatic solvents or biological systems, and that are difficult to tackle with other environment models, such as continuum solvation or QM/MM models.

ACKNOWLEDGMENTS

The authors thank The Netherlands Organization for Scientific Research (NWO) for financial support via the TOP program and gratefully acknowledge computer time provided by the Dutch National Computing Facilities (NCF).

¹ *Calculation of NMR and EPR Parameters. Theory and Applications*, edited by M. Kaupp, M. Bühl, and V. G. Malkin (Wiley-VCH, Weinheim, 2004).

² T. Helgaker, M. Jaszuński, and K. Ruud, *Chem. Rev.* (Washington, D.C.) **99**, 293 (1999).

³ M. Swart, C. Fonseca Guerra, and F. M. Bickelhaupt, *J. Am. Chem. Soc.* **126**, 16718 (2004).

⁴ J. Vollet, J. R. Hartig, and H. Schnöckel, *Angew. Chem., Int. Ed.* **43**, 3186 (2004).

⁵ J. Gracia, J. M. Poblet, J. Autschbach, and L. P. Kazansky, *Eur. J. Inorg. Chem.* **2006**, 1139 (2006).

⁶ M. Bühl, F. T. Mauschick, F. Terstegen, and B. Wrackmeyer, *Angew. Chem., Int. Ed.* **41**, 2312 (2002).

⁷ M. Profeta, F. Mauri, and C. J. Pickard, *J. Am. Chem. Soc.* **125**, 541 (2003).

⁸ C. Ochsenfeld, J. Kussmann, and F. Koziol, *Angew. Chem., Int. Ed.* **43**, 4485 (2004).

⁹ M. A. Watson, P. Sałek, P. Macak, M. Jaszuński, and T. Helgaker, *Chem.-Eur. J.* **10**, 4627 (2004).

¹⁰ P. Sherwood, in *Modern Methods and Algorithms of Quantum Comput-*

- ing, NIC Series Vol. 1, edited by J. Grotendorst (John von Neumann Institute for Computing, Jülich, 2000), pp. 257–277 (<http://www.fz-juelich.de/nic-series>).
- ¹¹ Q. Cui and M. Karplus, *J. Phys. Chem. B* **104**, 3721 (2000).
- ¹² J. Tomasi, B. Mennucci, and R. Cammi, *Chem. Rev. (Washington, D.C.)* **105**, 2999 (2005).
- ¹³ P.-O. Åstrand, K. V. Mikkelsen, P. Jørgensen, K. Ruud, and T. Helgaker, *J. Chem. Phys.* **108**, 2528 (1998).
- ¹⁴ R. Cammi, *J. Chem. Phys.* **109**, 3185 (1998).
- ¹⁵ B. Mennucci, J. M. Martínez, and J. Tomasi, *J. Phys. Chem. A* **105**, 7287 (2001).
- ¹⁶ B. Mennucci, *J. Am. Chem. Soc.* **124**, 1506 (2002).
- ¹⁷ M. Cossi and O. Crescenzi, *J. Chem. Phys.* **118**, 8863 (2003).
- ¹⁸ T. A. Wesolowski and A. Warshel, *J. Phys. Chem.* **97**, 8050 (1993).
- ¹⁹ T. A. Wesolowski, in *Computational Chemistry: Reviews of Current Trends*, edited by J. Leszczynski (World Scientific, Singapore, 2006) Vol. 10.
- ²⁰ Ch. R. Jacob, J. Neugebauer, L. Jensen, and L. Visscher, *Phys. Chem. Chem. Phys.* **8**, 2349 (2006).
- ²¹ M. Zbiri, C. A. Daul, and T. A. Wesolowski, *J. Chem. Theory Comput.* **2**, 1106 (2006).
- ²² J. Neugebauer, M. J. Louwerse, E. J. Baerends, and T. A. Wesolowski, *J. Chem. Phys.* **122**, 094115 (2005).
- ²³ J. Neugebauer, Ch. R. Jacob, T. A. Wesolowski, and E. J. Baerends, *J. Phys. Chem. A* **109**, 7805 (2005).
- ²⁴ J. Neugebauer, M. J. Louwerse, P. Belanzoni, T. A. Wesolowski, and E. J. Baerends, *J. Chem. Phys.* **123**, 114101 (2005).
- ²⁵ J. Neugebauer and E. J. Baerends, *J. Phys. Chem. A* **110**, 8786 (2006).
- ²⁶ M. Štrajbl, G. Hong, and A. Warshel, *J. Phys. Chem. B* **106**, 13333 (2002).
- ²⁷ M. H. M. Olsson, G. Hong, and A. Warshel, *J. Am. Chem. Soc.* **125**, 5025 (2003).
- ²⁸ M. Iannuzzi, B. Kirchner, and J. Hutter, *Chem. Phys. Lett.* **421**, 16 (2006).
- ²⁹ N. Govind, Y. A. Wang, A. J. R. da Silva, and E. A. Carter, *Chem. Phys. Lett.* **295**, 129 (1998).
- ³⁰ N. Govind, Y. A. Wang, and E. A. Carter, *J. Chem. Phys.* **110**, 7677 (1999).
- ³¹ T. Klüner, N. Govind, Y. A. Wang, and E. A. Carter, *Phys. Rev. Lett.* **86**, 5954 (2001).
- ³² T. Klüner, N. Govind, Y. A. Wang, and E. A. Carter, *J. Chem. Phys.* **116**, 42 (2002).
- ³³ T. A. Wesolowski, *Phys. Rev. Lett.* **88**, 209701 (2002).
- ³⁴ P. Huang and E. A. Carter, *J. Chem. Phys.* **125**, 084102 (2006).
- ³⁵ G. Vignale and M. Rasolt, *Phys. Rev. Lett.* **59**, 2360 (1987).
- ³⁶ E. Engel, in *Relativistic Electron Structure Theory, Part 1: Fundamentals*, edited by P. Schwerdtfeger (Elsevier Science, Amsterdam, 2002), Chap. 10, pp. 523–621.
- ³⁷ C. van Wüllen, in *Calculation of NMR and EPR Parameters. Theory and Applications*, edited by M. Kaupp, M. Bühl, and V. G. Malkin (Wiley-VCH, Weinheim, 2004), pp. 85–100.
- ³⁸ W. Kutzelnigg, in *Calculation of NMR and EPR Parameters. Theory and Applications*, edited by M. Kaupp, M. Bühl, and V. G. Malkin (Wiley-VCH, Weinheim, 2004), pp. 43–82.
- ³⁹ R. Ditchfield, *Mol. Phys.* **27**, 789 (1974).
- ⁴⁰ R. G. Parr and W. Yang, *Density-Functional Theory of Atoms and Molecules* (Oxford University Press, Oxford, 1989).
- ⁴¹ T. A. Wesolowski, *J. Chem. Phys.* **106**, 8516 (1997).
- ⁴² ADF, Amsterdam density functional program, Theoretical Chemistry, Vrije Universiteit Amsterdam, 2006 (<http://www.scm.com>).
- ⁴³ G. te Velde, F. M. Bickelhaupt, E. J. Baerends, C. Fonseca Guerra, S. J. A. van Gisbergen, J. G. Snijders, and T. Ziegler, *J. Comput. Chem.* **22**, 931 (2001).
- ⁴⁴ T. A. Wesolowski, H. Chermette, and J. Weber, *J. Chem. Phys.* **105**, 9182 (1996).
- ⁴⁵ T. A. Wesolowski, Y. Ellinger, and J. Weber, *J. Chem. Phys.* **108**, 6078 (1998).
- ⁴⁶ A. Lembarki and H. Chermette, *Phys. Rev. A* **50**, 5328 (1994).
- ⁴⁷ G. Schreckenbach and T. Ziegler, *J. Phys. Chem.* **99**, 606 (1995).
- ⁴⁸ A. D. Becke, *Phys. Rev. A* **38**, 3098 (1988).
- ⁴⁹ J. P. Perdew, *Phys. Rev. B* **33**, 8822 (1986).
- ⁵⁰ P. R. T. Schipper, O. V. Gritsenko, S. J. A. van Gisbergen, and E. J. Baerends, *J. Chem. Phys.* **112**, 1344 (2000).
- ⁵¹ O. V. Gritsenko, P. R. T. Schipper, and E. J. Baerends, *Chem. Phys. Lett.* **302**, 199 (1999).
- ⁵² O. V. Gritsenko, P. R. T. Schipper, and E. J. Baerends, *Int. J. Quantum Chem.* **76**, 407 (2000).
- ⁵³ J. Poater, E. van Lenthe, and E. J. Baerends, *J. Chem. Phys.* **118**, 8584 (2003).
- ⁵⁴ J. P. Perdew, J. A. Chevary, S. H. Vosko, K. A. Jackson, M. R. Pederson, D. J. Singh, and C. Fiolhais, *Phys. Rev. B* **46**, 6671 (1992).
- ⁵⁵ Ch. R. Jacob, T. A. Wesolowski, and L. Visscher, *J. Chem. Phys.* **123**, 174104 (2005).
- ⁵⁶ R. Cammi, B. Mennucci, and J. Tomasi, *J. Chem. Phys.* **110**, 7627 (1999).
- ⁵⁷ G. Merino, T. Heine, and G. Seifert, *Chem.-Eur. J.* **10**, 4367 (2004).
- ⁵⁸ T. Heine, C. Corminboeuf, and G. Seifert, *Chem. Rev. (Washington, D.C.)* **105**, 3889 (2005).
- ⁵⁹ C. Reichardt, *Solvents and Solvent Effects in Organic Chemistry*, 3rd ed. (Wiley-VCH, Weinheim, 2003).